Why the phosphotransferase system of Escherichia coli escapes diffusion limitation.

Francke, C.; Postma, P.W.; Westerhoff, H.V.; Blom, J.G.; Peletier, M.A.

published in
Biophysical Journal
2003

DOI (link to publisher)
10.1016/S0006-3495(03)74505-6

document version
Publisher's PDF, also known as Version of record

Why the Phosphotransferase System of *Escherichia coli* Escapes Diffusion Limitation

Christof Francke,*† Pieter W. Postma,* Hans V. Westerhoff,*†‡ Joke G. Blom,§ and Mark A. Peletier§¶
*BioCentrum Amsterdam, Swammerdam Institute for Life Sciences, University of Amsterdam, Amsterdam, The Netherlands; †BioCentrum Amsterdam, Department of Molecular Cell Physiology, Free University, de Boelelaan 1085, NL-1081 HV Amsterdam, The Netherlands; ‡Stellenbosch Institute for Advanced Study, Stellenbosch, South Africa; §CWI (Center for Mathematics and Computer Science), NL-1090 GB Amsterdam, The Netherlands; and ¶Eindhoven University of Technology, Eindhoven, The Netherlands

ABSTRACT We calculated the implications of diffusion for the phosphoenolpyruvate:glucose phosphotransferase system (glucose-PTS) of *Escherichia coli* in silicon cells of various magnitudes. For a cell of bacterial size, diffusion limitation of glucose influx was negligible. Nevertheless, a significant concentration gradient for one of the enzyme species, nonphosphorylated IIA^{Glc}, was found. This should have consequences because the phosphorylation state of IIA^{Glc} is an important intracellular signal. For mammalian cell sizes we found significant diffusion limitation, as well as strong concentration gradients in many PTS components, and strong effects on glucose and energy signaling. We calculated that the PTS may sense both extracellular glucose and the intracellular free-energy state. We discuss i), that the effects of diffusion on cell function should prevent this highly effective bacterial system from functioning in eukaryotic cells, ii), that in the larger eukaryotic cell any similar chain of mobile group-transfer proteins can neither sustain the same volumetric flux as in bacteria nor transmit a signal far into the cell, and iii), that systems such as these may exhibit spatial differentiation in their sensitivity to different signals.

INTRODUCTION

Many cellular processes involve the movement of pathway components to and from a membrane. Kinetic descriptions of such metabolic systems and signal transduction pathways tend to ignore the diffusion process, implicitly assuming that the spatial diffusion is fast relative to the reaction kinetics. However, a relatively straightforward analysis of an imaginary eukaryotic ''two-component system'', composed of a membrane-bound kinase and a cytoplasmic phosphatase, revealed that spatial gradients of phosphorylated and nonphosphorylated protein can be induced by signal-transducing flux within a mammalian cell (Brown and Kholodenko, 1999). These gradients might have significant control over the flux (Kholodenko et al., 2000). Essential to the phenomenon is the fact that here signal-transfer depends on the shuttling of a mobile protein and not on that of a metabolite.

Bacterial cells are much smaller than eukaryotic cells. A typical *Escherichia coli* B/r cell has dimensions of $\sim 1 \times 3$ μm (Nanninga, 1998), whereas a small eukaryote like baker's yeast (*Saccharomyces cerevisiae*) is already 4 μm in diameter (Sherman, 1991). Therefore, we wondered whether one should also expect an effect of diffusion on the functioning of important bacterial ''protein chains''. Instead of studying an imaginary system, we investigated the behavior of the PTS. In many bacteria, the PTS is responsible for the uptake and phosphorylation of various carbohydrates (Postma et al., 1993) at a very high rate (van der Vlag et al., 1995). On top of that, the protein components of the system play a diverse yet central role in the regulation of cellular activity in most of these organisms (see Lee et al., 2000; Lux et al., 1999; Seok et al., 1997; Tanaka et al., 2000; and reviews by Postma et al., 1993; Saier et al., 1996; Stülke and Hillen, 1999). Due to its spatial organization, the functioning of the PTS depends on diffusion: a phosphoryl group derived from cytoplasmic phosphoenolpyruvate is transferred by cytoplasmic proteins to a membrane protein that imports and phosphorylates the carbohydrate. This implies that a spatial gradient in the concentration of some of the protein species (be it phosphorylated, nonphosphorylated, or complexed) should build up for the pathway to develop flux. The main issue addressed here is how large such a gradient should be and whether it might lead to substantial fractional changes in local concentrations of PTS components, eventually limiting flux or signaling (diffusion limitation). A second issue treated is whether a similar system in a eukaryotic cell should be expected to develop gradients and diffusion limitation.

We set out to calculate this for the glucose-PTS of *E. coli* in a comprehensive manner, taking into account the spatial separation of the pathway components and the diffusion processes that are responsible for the transport to and away from the membrane. The parameter values in our model were based on experimental data only, combining the kinetic description of the glucose-PTS by Rohwer et al. (2000) and diffusion measurements in live *E. coli* (Elowitz et al., 1999). We show how *E. coli* escapes diffusion limitation of the metabolic and transport flux through this system in ways that are not available to the larger mammalian cell.

Submitted August 1, 2002, and accepted for publication January 21, 2003.

Dedicated to the memory of Dr. Pieter W. Postma, who died on April 21, 2002.

Address reprint requests to Christof Francke, Tel.: 0031-20-4447235; Fax: 0031-20-4447229; E-mail: cfrancke@bio.vu.nl.

Abbreviations used: PTS, phosphoenolpyruvate:carbohydrate phosphotransferase system; GFP, green fluorescent protein; glc, glucose; PEP, phosphoenolpyruvate.

0006-3495/03/07/612/11 $2.00

METHODS

Mechanism

The glucose-PTS of *E. coli* (discovered by Kundig et al., 1964) consists of four proteins: the general PTS-proteins enzyme I (EI) and HPr and the carbohydrate-specific proteins IIA^{Glc} and $IICB^{Glc}$. The former three proteins are located in the cytoplasm and relay a phosphoryl-group derived from phosphoenolpyruvate (PEP) in a consecutive manner to the latter membrane-bound protein, which in turn imports glucose and concomitantly phosphorylates it (Meadow et al., 1990; Postma et al., 1993; Robillard and Broos, 1999). Using the in vivo uptake rate of α-D-methyl glucoside (a glucose analog) of $\sim$0.9 nmol s^{-1} per mg dry cell weight (reported by van der Vlag et al., 1995), an in vivo $IICB^{Glc}$ concentration of $\sim$10 μM and a cellular volume of $\sim$2.5 μl per mg dry weight (cf. Rohwer et al., 2000), we calculate that $\sim$37 molecules of glucose are imported and phosphorylated per molecule of $IICB^{Glc}$ per s. Rohwer et al. (2000) made an in silicon replica of the glucose-PTS, i.e., a precise model exclusively based on the available literature data on K_m values, equilibrium constants, and association constants of the PTS-proteins for their substrates. Basic assumptions were that all elementary reactions in the pathway were bimolecular and that the reacting species were distributed homogeneously. Because the model ignored the spatiality of the pathway, we decided to make a new model that omits the latter assumption.

The explicit form of the modeled pathway is given in Fig. 1 and the model parameters in Table 1. The enzymes involved can occur in various states. Enzyme IIA^{Glc}, for instance, can either be nonphosphorylated (IIA^{Glc}), phosphorylated (IIA^{Glc}-P) or complexed (IIA^{Glc}-P-HPr and $IICB^{Glc}$-P-IIA^{Glc}). The term ''enzyme species'' will be used to refer to the different states throughout the text.

Diffusion and reaction rates

We assumed that reacting species meet through passive diffusion and that the diffusion process for every molecular species could be characterized by a single constant. The behavior of the molecules was modeled using a continuous representation (the concentration). The local change in the concentration of protein species p in time was related to the net production rate and diffusion rate by the balance equation:

$$\partial[p]/\partial t = v_p + \nabla \cdot (D_p \nabla[p]) \tag{1}$$

Equation 1 implies that the increase with time in a local concentration must equal the local net production rate (v_p) plus the net influx rate through diffusion. Convection was neglected because in the in vivo measurements of GFP movement, there were no indications of directional bias or enhanced apparent mobility (Elowitz et al., 1999; Dayel et al., 1999). Diffusion was parametrized by a protein specific diffusion constant D_p. ∇ is the operator for the spatial derivative and the precise formulation of $\nabla \cdot (D_p \nabla[p])$ thus depends on the dimension of the system and the coordinate system. Here ''local'' indicates a certain position in the cellular space for the cytoplasmic enzyme species, or on the membrane surface for the species situated at the membrane boundary.

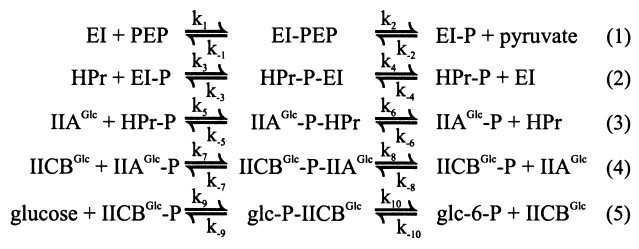

FIGURE 1 Reaction mechanism of the glucose-PTS of *E. coli*. In reaction 5, glucose comes from the periplasm, is phosphorylated, and the resulting glucose-6-phosphate is released into the cytoplasm, making the PTS an active uptake system for the glucose moiety. $IICB^{Glc}$ is a cytoplasmic membrane protein. All other components of the reaction scheme are cytoplasmic.

The net production rate v_p represents the sum of all rates that lead to the production of p minus all rates that lead to the consumption of p. The rate equations were derived directly from the reaction scheme in Fig. 1 (see Blom and Peletier, 2000, 2002). Because the concentrations [$IICB^{Glc}$], [$IICB^{Glc}$-P], [$IICB^{Glc}$-P- IIA^{Glc}], and [glc-P-$IICB^{Glc}$] are surface concentrations, their reaction rates were defined per unit of surface area.

For the mass balance of the cytoplasmic enzyme species, the reaction at the membrane represents a source/sink term. The corresponding boundary condition was obtained by equating the source/sink with the local flux near the membrane (direction represented by normal vector **n**). For IIA^{Glc} and IIA^{Glc}-P, the boundary condition yields Eqs. 2 and 3, and for the other cytoplasmic enzyme species Eq. 4:

$$D_{IIA}\ \partial[IIA^{Glc}]/\partial \mathbf{n} = k_8[IICB^{Glc}\text{-P-}IIA^{Glc}] - k_{-8}[IICB^{Glc}\text{-P}][IIA^{Glc}] \tag{2}$$

$$D_{IIA\text{-P}}\ \partial[IIA^{Glc}\text{-P}]/\partial \mathbf{n} = k_{-7}[IICB^{Glc}\text{-P-}IIA^{Glc}] - k_7[IICB^{Glc}][IIA^{Glc}\text{-P}] \tag{3}$$

$$D_p\ \partial[p]/\partial \mathbf{n} = 0 \tag{4}$$

The set of equations described in the above forms the core of our reaction-diffusion model.

Cell size, geometry, and numerical methods

E. coli cells are small cylinders with spherical poles. Depending on growth conditions and the strain, their diameter ranges from 0.5 to 1.5 μm and their length from 2 to 4 μm (Nanninga, 1998; Woldringh and Nanninga, 1985). One could describe the shape of the *E. coli* cell in various ways, such as cigar-like or rod-like. Because the latter term is used throughout biological literature, we will use rod or rod-like when describing the actual shape of the bacterial cell. We performed numerical experiments with a model rod cell with a diameter of 1.2 μm ($r = 0.6$ μm) and a length of 3 μm (see Blom and Peletier, 2002), and a spherical model cell with a radius (r) of 0.6 μm (see Blom and Peletier 2000). In all our calculations with both model cells, we found only a single steady state independent of the initial conditions and the lateral diffusion of the membrane component. Because the behavior of the system was essentially similar in both model cells, as described in the Appendix, we decided in this paper to treat the bacterial cell as if it were a sphere. This not only reduced the complexity of the description and the interpretation, but also made a straightforward comparison with a larger eukaryotic model cell possible. For a model mammalian cell, we assumed a sphere with a radius of 10 μm.

We considered all concentrations of cytoplasmic species to be functions of the spatial variable, and we confined the membrane-bound species to the boundary of the sphere. Because all solutions of our calculations were spherically symmetric, Eq. 1 can be reduced to the following system of reaction-diffusion equations:

$$\partial[c]/\partial t = v_c + (1/r^2)\partial((r^2 D_c)\partial[c]/\partial r)/\partial r \tag{1a}$$

for the cytoplasmic species c
and
for the membrane bound species m

$$\partial[m]/\partial t = v_m \tag{1b}$$

The concentrations of the cytoplasmic species were calculated using the resulting partial differential equations. For the membrane-bound species, these reduced to ordinary differential equations. The system was solved using the method of lines: the spatial derivatives were discretized on a computational grid and the resulting system of ordinary differential equations was integrated in time. We calculated the glucose flux (J) through

TABLE 1 Parameters of the reaction-diffusion model

Concentration of PTS proteins and boundary metabolites in μM			
$[EI]_{tot}$, $[HPr]_{tot}$: 5, 50		PEP/Pyruvate: 2800/900	
$[IIA^{Glc}]_{tot}$, $[IICB^{Glc}]^*_{tot}$: 40, 10		glucose/ glc-6-P: 500/50	
Rate constants odd, − even: (μM^{-1} s^{-1}); even, − odd: (s^{-1})			
k_1: 32.7	k_{-1}: 8000	k_6: 73.2	k_{-6}: 56.4
k_2: 1800	k_{-2}: 4.9	k_7: 14.7	k_{-7}: 14.7
k_3: 233.3	k_{-3}: 233.3	k_8: 44	k_{-8}: 16
k_4: 1400	k_{-4}: 56	k_9: 4.33	k_{-9}: 6.48
k_5: 366	k_{-5}: 366	k_{10}: 80	k_{-10}: $9\cdot10^{-5}$
Diffusion coefficients (μm^2 s^{-1})			
EI, EI-P(EP): 3.30		IIA-P-HPr: 4.37	
HPr-P-EI: 3.15		IIA, IIA-P: 5.00	
HPr, HPr-P: 6.30		Infinite: 2000	

The protein and boundary metabolite concentrations and rate constants were best estimates on the basis of the existing experimental data (see Rohwer et al., 2000). The tabulated diffusion coefficient of IIA^{Glc} was based on that found for GFP in *E. coli* by Elowitz et al. (1999). The other values were calculated from that using a molecular mass of 63.5, 9.1, and 18.1 kDa for EI, HPr, and IIA^{Glc}, respectively (de Reuse and Danchin, 1988).

*The $IICB^{Glc}$ concentration is given as a volume concentration. To obtain the surface concentration (in μm μM), the number was multiplied by the surface/volume ratio of the cell, which in the case of a spherical cell equals $3/r$.

the membrane with the aid of Eq. 5 when the system had reached a steady state:

$$J = 3/r \times (k_{10}[\text{glc-P-IICB}^{Glc}] - k_{-10}[\text{glc-6-P}][\text{IICB}^{Glc}]) \quad (5)$$

In this relation [glc-6-P] is interpreted as the concentration of glc-6-P at the membrane. Because the concentrations of $IICB^{Glc}$ and glc-P-$IICB^{Glc}$ are surface concentrations, we normalized by the surface/volume ratio (i.e., $(4\pi r^2)/(4/3\pi r^3)$) to obtain the volume flux J. For a more detailed description of the numerical methods used, readers are referred to Blom and Peletier (2000, 2002).

Parameters and variables

Rate constants and enzyme concentrations were taken from Rohwer et al. (2000) and references cited therein. The membrane concentration of $IICB^{Glc}$ was calculated from the bulk-projected concentration by multiplying the bulk concentration with the volume/surface ratio. The PEP and pyruvate concentrations were taken from Hogema et al. (1998), who determined these in glucose-grown cells. Four different combinations of glucose and PEP concentrations were used to evaluate their influence. The lower PEP concentration was chosen such that it was below the K_m ($K_{m,\,PEP} = 300$ μM (Rohwer et al., 2000)). The glucose concentrations were chosen such to be either at saturation or below the K_m ($K_{m,glucose} = 20$ μM (Rohwer et al., 2000)).

In our calculations, the concentrations of the metabolites PEP, pyruvate, glucose-6-phosphate, and glucose were treated as constant parameters. In general the concentrations of intracellular metabolites are much higher than those of the intracellular proteins and are controlled by many processes. As a result, metabolite concentrations remain constant in the cell, at least for certain periods of time, independent of changes in the activity of one of the producing or consuming processes. Moreover, in our case, steady state was obtained within a fraction of a second, allowing only small eventual changes in metabolite concentrations. From a comparison of the cell density, the cellular volume, the diffusion rate of glucose in water (~670 μm^2 s^{-1} (Weast, 1975)), the glucose concentration, and the glucose uptake rate (van der Vlag et al., 1995), we do not expect any diffusion limitation of glucose on the outside of the model cells.

We assumed a diffusion constant for IIA^{Glc} of 5 μm^2 s^{-1}. The diffusion rate of the GFP (27 kDa) in the cellular matrix of *E. coli* has been determined experimentally by Elowitz et al. (1999). It was measured in elongated *E. coli* cells by means of fluorescence recovery after photobleaching and the reported values range from 3.6 to 7.7 μm^2 s^{-1}. The lower rate was found in cells with a high GFP expression level and probably identifies the diffusion rate of GFP dimers (54 kDa). Protein diffusion in the cytoplasm of *E. coli* cells thus was two- to fourfold slower than in the eukaryotic endoplasmic reticulum or mitochondrion, respectively, and about five times slower than in eukaryotic cytoplasm (Dayel et al., 1999). To establish the possible effects of diffusion on the behavior of our bacterial transport system, we decided to use the lower number reported by Elowitz et al. (1999) because this value seems to present a lower limit to the rate of ''free'' protein diffusion in vivo.

The diffusion coefficients of the other PTS ''enzyme species'' were calculated from that of enzyme IIA^{Glc} assuming that: i), all enzyme species are spheres, ii), the diffusion coefficient varies linearly with the inverse of the radius of that sphere, and iii), the volume of the sphere varies proportionally with the mass of the protein species. A situation in which all cytoplasmic enzyme species are distributed homogeneously was simulated by making the diffusion coefficient 2000 μm^2 s^{-1} (~infinite) for all species.

Signal

In the PTS, not only the protein components diffuse between membrane surface and cytoplasm, but also the phosphoryl-group. The latter does this by playing ''piggyback'' on the components of the PTS. Looking at the PTS as a signal relay chain, we define the local concentration of the PTS signal (σ) as the sum of local concentrations of the phosphorylated mobile PTS components minus the sum of the local concentrations of the nonphosphorylated mobile PTS components:

$$[\sigma] = [\text{EI-P}] + [\text{HPr-P}] + [\text{IIA}^{Glc}\text{-P}] - [\text{EI}] - [\text{HPr}] - [\text{IIA}^{Glc}] \quad (6)$$

For signal to transfer at steady state, a phosphorylated protein must diffuse to the membrane and a nonphosphorylated protein must diffuse back. Because the intermediary protein complexes can be considered to carry both a phosphorylated as well as a nonphosphorylated enzyme, diffusion of these complexes does not contribute to the signal diffusion.

RESULTS

Estimated concentration gradients

Brown and Kholodenko (1999) showed that in mammalian cells, gradients of active forms of signal transduction proteins may arise. Their approximate argument can be recalculated for the case of the *E. coli* PTS. If the signal protein is dephosphorylated at the plasma membrane and rephosphorylated in the center of the cell, a gradient of the nonphosphorylated form of the protein must exist to drive the diffusion. The concentration difference ($\Delta[p]$) and the flux (J) are then related by Fick's first diffusion equation. For a spherical cell this reads:

$$\Delta[p] = {}^1/_3\, Jr^2/D \quad (7)$$

Inserting a flux of 0.37 mM s^{-1} (Rohwer et al., 2000), a diffusion coefficient (D) of 5 $\mu m^2\ s^{-1}$ and a radius (r) of 0.6 μm, one finds a concentration difference between cell center and membrane surface of 9 μM. Such a gradient should be quite significant for PTS proteins, which occur at concentrations between 5 and 50 μM (see Table 1). A cell radius of 10 μm leads, in the case of similar flux, to the enormous concentration gradient of ~2.5 mM (over 10 μm) by the same calculation, and of ~0.5 mM if diffusion is assumed to be five times faster, as prevalent in eukaryotic cytoplasm (Dayel et al., 1999). These estimated concentration differences are much higher than the total concentration of the PTS proteins, which amounts to only 0.1 mM. The difference in signal concentration, as expressed in $[\sigma]$ (Eq. 6), between membrane surface and the cell center should be even double these numbers, because an inverse gradient will exist for the phosphorylated proteins. This indicates that in larger cells, diffusion should interfere with the functioning of a system such as the PTS.

The above estimations (cf. Fig. 3 *A*, *open triangles*) suggested that substantial gradients will be present in the active PTS. The PTS is a multicomponent system, however, in which both phosphorylated and nonphosphorylated forms of each protein may diffuse. The concentrations of these forms depend on the PTS activity. In addition, not all rephosphorylation of EI occurs in the center of the cell; PEP diffuses throughout the cytoplasm. Consequently, a more comprehensive calculation was required to see whether spatial limitations are indeed as prohibitive as suggested by the preliminary calculations described in this section.

Calculated gradients for bacterial cells

As a point of reference, we first calculated both the PTS flux and the concentration distribution of the four PTS enzymes over their different states in the case of extremely fast diffusion of the cytoplasmic species. The results are listed in column 2 of Table 2 and are identical to those reported by Rohwer et al. (2000).

We then recalculated the flux and spatial distribution of the enzyme species for cells with a radius of 0.6 μm using realistic values for the diffusion coefficients. The results are shown in columns 5 and 6 of Table 2 and in Fig. 2. The effect of the less than infinitely fast diffusion on the flux was remarkably small, i.e., <1%. Likewise, the gradients that developed in the concentrations of components of EI of the PTS were small, concentration differences between the center of the cell and close to the membrane remaining below 4%. Defining the signal in terms of the concentration difference of phosphorylated and nonphosphorylated uncomplexed PTS protein (Eq. 6), the signal concentration difference between membrane surface and cell center was ~5 μM. This was some four times smaller than the first-order estimate of 20 μM using Fick's diffusion equation (see earlier). An important reason for this difference is that rephosphorylation of EI occurred throughout the cell rather than being confined to the cell center. The signal concentration difference was mainly distributed over HPr and IIA^{Glc}, the proteins present at higher concentrations.

Although the concentration of both enzymes HPr and IIA^{Glc} was high with respect to that of the signal, the phenomenon that each PTS protein was rather unevenly distributed over its subforms meant that some of those subforms could be subject to significant concentration gradients. Quite notably, this was the case for nonphosphorylated IIA^{Glc}: its concentration was more than 35% higher near the membrane than in the cell center or than the cell average. The steady-state concentration of nonphosphorylated IIA^{Glc} did not vary linearly with distance from the membrane, but increased sharply near the membrane (see Fig. 2, *right*). The ratio of IIA^{Glc}-P/IIA^{Glc} changed even more drastically.

We explored the role of the individual diffusion constants by reducing them one by one severalfold (not shown). When we looked at the effect on flux we saw that reduction in the movement of IIA^{Glc}-P brought about a decrease in the flux: a 10-fold slowing down led to a 7% flux reduction. A 10-fold decrease of the other diffusion constants did not influence the flux markedly. Similar changes in the diffusion rate of the HPr and IIA^{Glc}-related species led to significant concentration gradients for those species whose diffusion was being retarded and for nonphosphorylated IIA^{Glc}, whereas for EI-related species nothing happened upon reduction of the diffusion rates. A detailed analysis of the diffusion control of glucose flux mediated by the PTS is described elsewhere (Francke et al., 2002).

Gradients and diffusion limitation in cells of various sizes

We next modified the radius of our model cell to 0.3 and 10 μm, keeping the volume-averaged concentrations of total EI, HPr, IIA^{Glc}, and $IICB^{Glc}$ constant. We again calculated the flux through the pathway and the concentration distribution of the four enzymes over their different states and over the cellular space (cf. columns 3 and 4, and 7 and 8 of Table 2, respectively). As expected, decreasing the radius of the cell from 0.6 to 0.3 μm did not affect the flux through the glucose-PTS. The concentration difference between nonphosphorylated IIA^{Glc} in the center of the cell and nonphosphorylated IIA^{Glc} near the membrane lost significance by decreasing to 15%. This is in line with the squared dependence of the concentration gradients on the radius of the cell predicted by Eq. 7.

Clearly in the smallest cell considered, diffusion limitation lacked significance. This pinpointed that cell size might be a major factor determining whether or not concentration gradients and flux limitation by diffusion arise in the bacterial PTS. That this was indeed the case is illustrated

TABLE 2 Flux and distribution of the glucose-PTS protein species in cells of different radii

		$r = 0.3$ μm		$r = 0.6$ μm		$r = 10.0$ μm	
1.	2. $D_c = \infty$	3. c	4. m	5. c	6. m	7. c	8. m
EI	0.27	0.27	0.27	0.27	0.27	0.27	0.27
EI-PEP	3.05	3.05	3.05	3.05	3.05	3.06	2.95
EI-P	1.19	1.19	1.19	1.20	1.19	1.25	1.01
HPr-P-EI	0.49	0.49	0.49	0.48	0.50	0.43	0.79
HPr	1.28	1.25	1.28	1.12	1.33	0.34	4.53
HPr-P	29.8	30.1	29.7	31.0	29.2	40.1	16.7
IIA-P-HPr	18.5	18.0	18.6	16.9	19.3	7.69	35.1
IIA	0.64	0.60	0.74	0.55	0.87	0.19	3.69
IIA-P	15.4	15.9	15.2	16.9	14.5	29.1	1.58
IICB-P-IIA	5.47		5.46		5.43		2.48
IICB	1.41		1.43		1.49		6.14
IICB-P	0.12		0.12		0.12		0.05
glc-P-IICB	2.99		2.99		2.97		1.33
σ(signal)		45.1	43.8	47.2	42.4	69.6	10.8
$-\Delta\ \sigma$ (m $-$ c)			1.3		4.8		58.8
σ_c/σ_m			1.0		1.1		6.4
J	240		239		237		106

Column 2 was obtained assuming a diffusion constant of 2000 $\mu m^2\ s^{-1}$ for all species. For realistic diffusion coefficients, we arrived at the numbers of columns 3–8. For every radius, the first column gives the concentrations near the center of the cell and the second one those near the membrane boundary. The concentrations are given in μM, the flux in $\mu M\ s^{-1}$.

by Fig. 3 *A*, where the PTS flux is represented as a function of the radius of our spherical model cell. The dark and light gray areas indicate the regions of the plot that may be relevant for bacterial and mammalian cells, respectively. Fig. 3 *A* also shows the corresponding signal concentration difference between membrane and bulk. Fig. 3 *B* shows the concentration of IIA^{Glc} in the cell center relative to that near the membrane (*open circles*) and vice versa for IIA^{Glc}-P (*closed circles*). From Fig. 3 it is apparent that whereas the cell radius only affected the flux due to diffusion limitation at the highest cell sizes, an effect on signal transduction through the concentrations of phosphorylated and nonphosphorylated IIA^{Glc} (and their ratio) should already be expected for cells the size of *E. coli* or only slightly larger, or with only slightly hampered diffusion.

As can be seen in Table 2 and Fig. 3 *B*, in cells with a radius of 10 μm, nonphosphorylated IIA^{Glc} was subject to a dramatic concentration gradient; its concentration at the membrane surface was almost 20 times that in the cell center. For HPr, a 13-fold, for HPr-P a 0.4-fold, for HPr-P-IIA^{Glc} a 4.5-fold, and for IIA^{Glc}-P a 0.05-fold concentration ratio was calculated between the membrane and the center of the cell. In these cells the flux was reduced by ~55%. The difference in signal concentration between membrane surface and cell center amounted to 59 μM, getting closer to its theoretical maximum of 95 μM, i.e., the total cell-averaged concentration of PTS components. Again the diffusion gradients were distributed over more than one component and concentrated in components that were present at higher

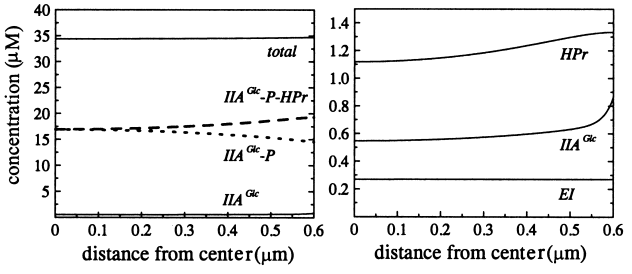

FIGURE 2 The concentration distribution of the IIA^{Glc}-related (*left panel*) and nonphosphorylated cytoplasmic enzyme species (*right panel*) in a cell with radius 0.6 μm in the presence of both PEP (2.8 mM) and glucose (500 μM).

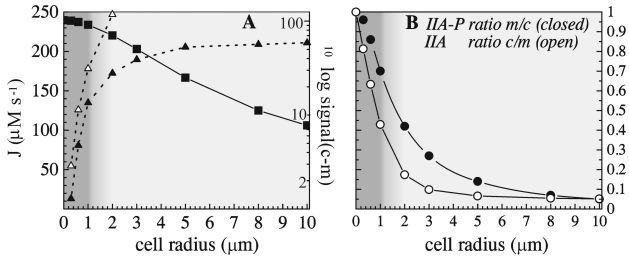

FIGURE 3 Cell size affects flux and concentration gradients. (*A*) Flux through the PTS (*left ordinate*, *squares*), and the difference in signal concentration between cell center and inner membrane as a function of cell radius (*right ordinate*, *triangles*). The open triangles represent a rough estimate based on Eq. 7 and the calculated flux, and the closed triangles represent the result of the precise calculation using Eq. 6 (note that the scale is logarithmic). (*B*) The concentration ratio of phosphorylated IIA^{Glc} (*closed circles*, *membrane/center*) and of nonphosphorylated IIA^{Glc} (*open circles*, *center/membrane*). The dark gray area is relevant for bacterial dimensions, the light gray area for eukaryotic cells.

total concentrations. EI-related enzyme species were not subject to concentration gradients of any significance, with the exception of its complex with HPr. For $IICB^{Glc}$, the amount of nonphosphorylated enzyme began to rise and the amount of phosphorylated species and complexes began to drop as the cell radius exceeded 0.6 μm. These changes correlated with the decrease in flux.

Phosphorylation state of IIA^{Glc}: glucose and free-energy sensing

Enzyme IIA^{Glc} and IIA^{Glc}-P are considered sensors for glucose (Postma et al., 1993; Saier et al., 1996; Stülke and Hillen, 1999). We mimicked the absence of glucose by lowering its concentration from 500 to 0.5 μM. In case diffusion was infinitely fast and in the presence of PEP, the concentration of phosphorylated IIA^{Glc} rose twofold and that of nonphosphorylated IIA^{Glc} more than halved when glucose was removed, thus confirming that the concentration of these species responded significantly to the glucose signal. Changes in the cellular free-energy state, as reflected in the PEP concentration, induced a similar yet inverse response. The low PEP concentration applied (90 μM) has been found in cells ~15 s after *E. coli* cells started importing glucose (Hogema et al., 1998).

When we used realistic values for the diffusion constants, both nonphosphorylated and phosphorylated IIA^{Glc} continued to respond to changes in extracellular glucose concentration as well as to changes in PEP levels (as depicted in Fig. 4, *top*). In addition, concentration gradients for both phosphorylated and nonphosphorylated IIA^{Glc} were found. The same response was calculated for mammalian model cells but only within a micron distance from the membrane (depicted in Fig. 4, *bottom*). Further away from the membrane it looked as if the concentrations of nonphosphorylated and phosphorylated IIA^{Glc} were influenced only by the concentration of PEP. Thus, in fact, in these larger cells, the glucose signal ceased to exist after ~1 μm on its way into the cell. When we assumed diffusion to be five times faster, as is the case in eukaryotic cytoplasm (Dayel et al., 1999), this distance increased only to ~1.5 μm (not shown). In the right panels of Fig. 4, a change in the relative ordering of the lines corresponding to low PEP concentration seems to have occurred. However, if one compares both graphs on the same spatial scale, i.e., one compares the top graph with the rightmost 0.6 μm of the bottom graph, then it becomes clear that the crossover in concentration occurs at too large a distance from the membrane to persist in the smaller cell of the top graph.

IIA^{Glc} "senses" the concentration of PEP via two intermediate proteins, i.e., EI and HPr. We wondered what would happen should these be removed. The model was therefore slightly adjusted by fixing the concentrations of phosphorylated and nonphosphorylated HPr and setting their concentrations to 2.8 and 0.9 mM, respectively, identical to those of

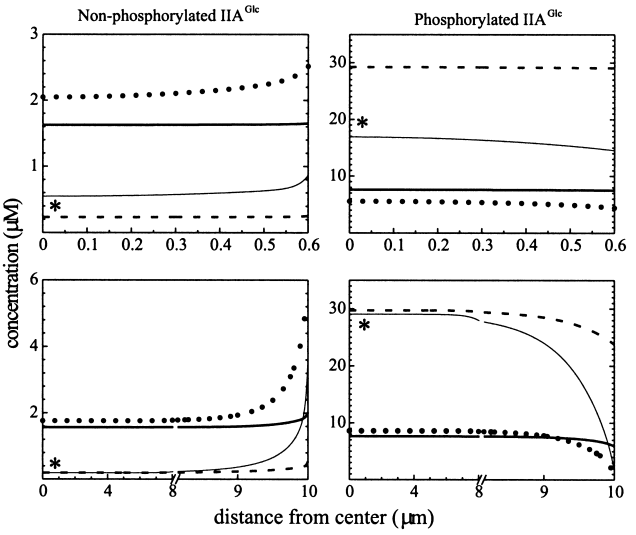

FIGURE 4 Position dependent response to glucose and free energy. The concentration distribution of nonphosphorylated IIA^{Glc} and phosphorylated IIA^{Glc} in cells with radius 0.6 μm (*top*) and 10 μm (*bottom*) under various conditions of metabolite availability; 2800 μM PEP and 0.5 μM glucose (*dashed line*); 2800 μM PEP and 500 μM glucose (*thin solid line*, indicated by *asterisk*); 90 μM PEP and 500 μM glucose (*dotted line*); and 90 μM PEP and 0.5 μM glucose (*thick solid line*).

the original phosphoryl-donor PEP and pyruvate. Therewith our model became representative of a two-protein PTS. At the initial parameter settings, this system hardly phosphorylated glucose because of the relatively high affinity of IIA^{Glc}-P for HPr (now pyruvate) and the 20-fold higher concentration of the latter, leaving nearly no free IIA^{Glc}-P. Therefore we changed the rate constants of the association and dissociation reactions between PEP/pyruvate and IIA^{Glc} so that they became equivalent to those between EI and PEP, i.e., k_5, k_{-5}, k_6, and k_{-6} were replaced by k_1, k_{-1}, k_2, and k_{-2}, respectively (cf. Table 1). In this way, a high glucose phosphorylation flux was restored but now the concentrations of phosphorylated and nonphosphorylated IIA^{Glc} became insensitive to the glucose concentration and only responded to changes in the PEP concentration. Thus IIA^{Glc} would loose its signaling function for glucose. The reason for the insensitivity toward glucose might be the large concentration difference between the main actors (PEP and glucose) that influence the IIA^{Glc} phosphorylation state.

Resensitization of the phosphorylation state of IIA^{Glc} for glucose was achieved by decreasing the association rate constants of nonphosphorylated IIA^{Glc} with PEP and phosphorylated IIA^{Glc} with pyruvate, decreasing the dissociation rate constants of the formed IIA^{Glc}-PEP complex, and simultaneously increasing the dissociation rate constants (k_{-7} and k_8) of the $IICB^{Glc}$-P-IIA^{Glc} complex, all 100-fold. Indeed, such a decrease in the association and dissociation rate constants of the protein metabolite complex IIA^{Glc}-PEP and an increase in the dissociation rate of the protein-protein complex $IICB^{Glc}$-P-IIA^{Glc}, rendered the phosphorylation

state of the signaling protein IIA^{Glc} sensitive to both glucose and PEP throughout the cell while maintaining a realistic glucose influx at both high and low PEP concentration. In this particular case, however, the association rate constants for nonphosphorylated and phosphorylated IIA^{Glc} with PEP and pyruvate would be about two orders of magnitude smaller than the association rate constants for phosphorylated and nonphosphorylated IIA^{Glc} with $IICB^{Glc}$ and $IICB^{Glc}$-P. Such a difference in association rate constants between the protein-metabolite complex IIA^{Glc}-PEP and the protein-protein complex $IICB^{Glc}$-P-IIA^{Glc} is highly unlikely considering the fact that the nature of the association in these phosphoryl-transfer complexes is nearly identical, with similar changes in free energy for the phosphoryl transfer, and the fact that the diffusion rate of the metabolites PEP and pyruvate is much higher than that of IIA^{Glc}. Moreover, a large increase in the dissociation rate constants of the $IICB^{Glc}$-P-IIA^{Glc} protein-protein complex with respect to those we used, and which were determined in vitro, is rather improbable in the crowded environment of the cell because crowding reduces dissociation rates of protein-protein complexes instead of increasing them (Rohwer et al., 1998b).

DISCUSSION

Most models of metabolic and signal-transduction pathways describe the cell as a ''well-stirred reactor'', its soluble components distributed homogeneously throughout. To investigate whether this is actually to be expected, we developed a reaction-diffusion model of the glucose-PTS of *E. coli*, a well-characterized multi component transport and signal transduction system exhibiting a very high membrane flux.

For a cell of bacterial size (diameter of 0.6 μm or smaller), we found that neither glucose flux nor the spatial distribution of most PTS enzyme species were affected when relaxing the usual assumption that diffusion was infinitely fast. This lack of effect was at first unexpected, because a simplified calculation suggested that a concentration gradient much in excess of the concentration of EI should arise. Our model revealed that the actual concentration gradient in signal was some three times smaller, still close to the total concentration of EI. However, most of the concentration gradient was carried by the more abundant enzymes HPr and IIA^{Glc}. Apparently potential diffusion limitation in a phospho-relay chain can be prevented by having one or more of the participating proteins present at a sufficiently high concentration.

The relationship we found between flux and the total concentration of the different enzymes (not shown) was similar to that reported in vivo (van der Vlag et al., 1995) and obtained with the kinetic model of Rohwer et al. (2000) (cf. Fig. 1 of this reference). When we compared the individual enzyme species, we saw that the diffusion of EI, HPr, and related species hardly affected the behavior of the glucose-PTS. It seemed as if nonphosphorylated and phosphorylated IIA^{Glc} performed nearly all of the diffusion labor (see also Francke et al., 2002). In this, nonphosphorylated IIA^{Glc} was most apt to form concentration gradients and phosphorylated IIA^{Glc} was by far the most important species sustaining the inward flux of glucose and the delivery of the phosphoryl groups toward the membrane. In fact, this role for IIA^{Glc} was not without consequences. Already in cells with radius 0.6 μm, the concentration of nonphosphorylated IIA^{Glc} was subject to diffusion limitations: An appreciable concentration difference developed between the membrane and the cell center due to the influx of glucose. Contrary to what is generally assumed (Postma et al., 1993; Saier et al., 1996), the calculations also suggest that in the presence of both glucose and PEP, there should be relatively little nonphosphorylated EI, HPr, and IIA^{Glc}. The presence of nonphosphorylated IIA^{Glc} at such relatively low concentrations (as compared to IIA^{Glc}-P) made it more susceptible to concentration changes/gradients.

The effect of diffusion on the concentration of nonphosphorylated IIA^{Glc} is potentially important, as it is this enzyme species that is responsible in *E. coli* for much of one of the most pleiotropic regulatory effects in bacteria, i.e., glucose or catabolite repression (Stülke and Hillen, 1999). Nonphosphorylated IIA^{Glc} interacts with various non-PTS sugar transport proteins in a process called inducer exclusion (Misko et al., 1987; Nelson et al., 1982; Novotny et al., 1985; Osumi and Saier, 1982; Postma et al., 1984; Saier et al., 1983). Upon binding of IIA^{Glc}, the activity of the transport protein is reduced and the import of several non-PTS carbon sources as well as the consequent induction of gene expression of genes related to their transport and metabolism is prevented (see Postma et al., 1993). Because these proteins are mostly, if not all (Voegele et al., 1993), located at the membrane, the effect of diffusion will be that it enhances the inhibition of these proteins under flux conditions by raising the concentration of nonphosphorylated IIA^{Glc} near the membrane.

Normally the relative amounts of IIA^{Glc} and proteins binding IIA^{Glc} are such that the flux through the PTS is maximal. But on the rare occasion that the relative amount of IIA^{Glc} is low, the flux can be reduced by its binding to non-PTS proteins, a phenomenon that is called ''reverse inducer exclusion'' (van der Vlag et al., 1994; Rohwer et al., 1998a). When the majority of the IIA^{Glc} is bound, its effective diffusion coefficient should be reduced, and then even in very small cells, flux could cause concentration gradients.

Including the effects of macromolecular crowding on the PTS (as reported by Rohwer et al., 1998b) should lead to a further decrease in the concentrations of uncomplexed PTS components such as IIA^{Glc}. Assuming then that nonphosphorylated IIA^{Glc}, and not any of its complexes, is responsible for inducer exclusion, this should mean that the effects of diffusion limitation on inducer exclusion should be even stronger in crowded reality than in our uncrowded model.

Enzyme IIA^{Glc} of *E. coli* mediates another signal transduction route also effecting glucose repression. At low glucose (and high PEP), many catabolic operons are activated by the action of cAMP (Botsford and Harman, 1992). The cAMP is produced by adenylate cyclase, and that enzyme is activated by phosphorylated IIA^{Glc} (Saier et al., 1996). In our calculations the effects of diffusional limitation on the concentration of phosphorylated IIA^{Glc} are much smaller, in relative terms, than the effects on nonphosphorylated IIA^{Glc}. As a consequence diffusion limitation may affect the inducer exclusion mechanism of catabolite repression more strongly than the cAMP-mediated mechanism.

A point of concern might be that the results of our calculations depended to some extent on the diffusion coefficient that was applied. Because the effects of diffusion are inversely proportional to the square of the cell radius, increasing the diffusion coefficient is phenomenologically equivalent to reducing the cell radius. Behavior displayed by the PTS in a cell at a certain rate of diffusion will be observable in a proportionally bigger cell at a higher diffusion rate. The above implies that our findings will hold irrespective of the precise choice of the diffusion coefficient. In fact, the results appeared not very sensitive to the precise magnitude of the diffusion coefficient; only order of magnitude changes induced marked effects.

Our calculations show that in a bacterial cell, the phosphorylation state of IIA^{Glc} is sensitive to both the presence of glucose and the free-energy status of the cell (in the form of PEP), and thus presents sort of a dual sensing mechanism. ''Starved'' *E. coli* cells have an elevated PEP concentration (Hogema et al., 1998). This ''standby'' condition is the one that gives rise to the dashed lines in Fig. 4. As a consequence of this condition, glucose repression should be minimal along either of its routes (e.g., mediated via inducer exclusion or via cAMP). In this way the cell is able to take up and metabolize any carbohydrate that happens to be available. Addition of glucose should activate both repression mechanisms somewhat, although incompletely, and this is illustrated by the thin solid lines (marked by an asterisk) of Fig. 4. Whereas in the cAMP-mediated glucose repression, effects of the cellular free-energy state have been invoked (e.g., through cAMP efflux at high free-energy states (Makman and Sutherland, 1965; Saier et al., 1975)), inducer exclusion was mainly perceived as a sugar-mediated repression mechanism and not as a free-energy checking mechanism (Postma et al., 1993; Saier et al., 1996; Stülke and Hillen, 1999). Consequently, the calculated result that free-energy (or rather PEP) depletion (*dotted* and *thick solid lines*) in itself should cause stronger inducer exclusion than glucose addition might come as a surprise. On the other hand, both the PEP/pyruvate ratio (Weigel et al., 1982) and the ATP/ADP ratio (Rohwer et al., 1996) were implied in the regulation of PTS activity. And Hogema et al. (1998) established a correlation between the phosphorylation state of IIA^{Glc} and the PEP/pyruvate ratio. In fact, the strong inducer exclusion effect consequent to glucose addition to starved cells (Postma et al., 1993; Saier et al., 1996) may consist of a direct effect of glucose plus an indirect effect through a reduction in the intracellular PEP concentrations.

The right panel of Fig. 4, *top*, showed that also the phosphorylated form of IIA^{Glc}, which directs the cAMP-mediated glucose repression mechanism, is sensitive to both glucose and loss of free energy in the form of PEP. In terms of absolute concentrations, the response of IIA^{Glc}-P was some five times stronger than that of IIA^{Glc}.

In larger cells, we observed rather curious phenomena, i.e., spatial differentiation of the dual sensing mechanism: close to the membrane IIA^{Glc} and IIA^{Glc}-P became primarily responsive to glucose, whereas away from the membrane both became exclusively responsive to the cellular free-energy state as projected into the PEP concentration. The explanation for this is the long diffusion path, semi-isolating the membrane part of the PTS from the cytosolic part. In cells of bacterial size, there is some tendency toward the same phenomena and any additional diffusion limitation due to, for instance, macromolecular crowding near that membrane should enhance the effect.

Sustenance of glucose and PEP sensing properties, although maintaining a realistic glucose influx, appeared difficult the moment we turned the four-enzyme PTS into a two-enzyme PTS, consisting of only enzymes IIA^{Glc} and $IICB^{Glc}$. This was probably due to incompatibility between the flux requirements and the large concentration differences between the metabolites and the enzymes. The outcome suggests that EI and HPr function as some sort of attenuator for the intracellular energy signal, such that IIA^{Glc} can respond to concentration changes in both glucose and PEP in a concerted manner, rather than that it responds to PEP only. It is interesting in this respect that our calculations for the ''normal'' PTS also show that the concentrations of phosphorylated and nonphosphorylated EI react solely to changes in the PEP concentration, whereas Lux et al. (1999) suggest that the chemotactic response toward PTS sugars, which is supposedly triggered by dephosphorylation of EI (Lengeler and Jahreis, 1996), is an immediate effect of the presence of the sugar. Assuming our model is right, this can only be when PEP levels are compromised simultaneously.

According to our model, ordinarily the effects of diffusion on the PTS flux should be negligible in cells the size of *E. coli*. For cells with diameters exceeding 2 μm, however, the control by diffusion on flux became significant. Also many of the PTS proteins began to differ in concentration between membrane surface and cell center. Thus, considering the fact that most enzyme species are involved in other pathways, variable cellular activities can be envisaged in such cells, mediated by the large local concentration differences of these species. It may be telling that possibly the largest organism that contains a PTS, *Bacillus megatherium*, with an average size of 4 μm $\times$ 1.5 μm (Gordon, 1974), still falls within the range of cells that should not be subject to PTS flux

limitation, or substantial gradients in all but one of the species.

Most eukaryotic cells are much larger than bacteria and completely lack the PTS. Until now it has remained unclear why these larger organisms lack this highly effective carbohydrate import system. For glucose uptake, many eukaryotes rely on a facilitated diffusion carrier, intracellular glucose carrying out the required diffusion. Perhaps the limitation by diffusion on PTS performance in larger cells is what prevents its effective use in eukaryotes. Here we should make two reservations: i), in our calculations, we increased the cell diameter while keeping the volumetric flux of the PTS constant, i.e., we increased the glucose influx per cell with the third power of the radius (in case diffusion was neglected); and ii), intracellular signaling of the external glucose concentration was impaired only over distances larger than, say, 0.3–0.5 μm, in other words the system would be capable of signaling both glucose and PEP over short distances within the eukaryotic cell.

The PTS has the triple function of catalyzing carbohydrate phosphorylation and uptake, as well as mediating glucose signaling. The former two processes require high flux capacity, the third much less so. Accordingly, it is only the flux function of the PTS that may be incompatible with eukaryotic cell size, not the signal transduction function. Indeed, whereas in eukaryotes metabolic flux and signaling seem to have been separated and metabolic phosphoryl-flux is mediated by low molecular mass carriers such as creatine and ADP rather than by proteins, signal transduction is still mediated by proteins. However, the mechanism of this signal transduction is catalytic in terms of activating kinases that take the signal phosphate from ATP. Only little of the amount of signal generated in, for instance, the nucleus actually diffuses from the plasma membrane through these kinase chains, whereas in phospho-relay chains such as the PTS, all the signal diffuses. Our results (cf. Fig. 4, *bottom*) make it clear that a PTS-like phospho-relay chain would fail miserably in transferring a signal from the membrane to the inside of a large cell, because already within a relatively short traveling distance ($\sim$1 μm), the signal related to the status near the membrane should be lost and replaced by a signal that is representative of the status inside the cell. For quite a while, the function of the protein kinase cascades has been assumed to be signal amplification in terms of high response coefficients (Goldbeter and Koshland, 1982), but the rationale for this has recently been put into question (Ortega et al., 2002). Perhaps the primary functionality of the kinase cascade structure of these chains is their ability to prevent this loss of signal in a way that resembles action potential propagation or the signal transport along telephone networks.

Model calculations are only as valid as the underlying kinetic scheme and its assumed parameter values. Consequently, our results should be taken as indicative only for the implications of diffusion for signal transduction by phospho-

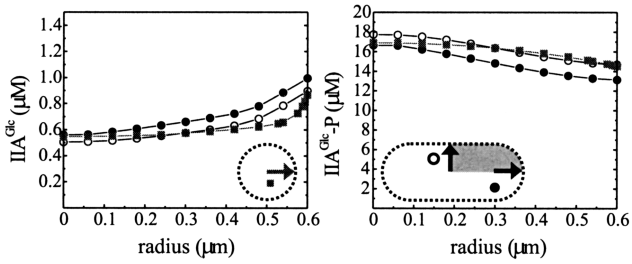

FIGURE 5 The concentration distribution of nonphosphorylated (*left*) and phosphorylated IIA^{Glc} (*right*) in a spherical cell with radius 0.6 μm (*squares*), and in a rod-like cell with length 3 μm. The distribution in the latter is represented along two lines of length 0.6 μm perpendicular to the membrane boundary. These lines represent the two extremes found in the rod, i.e., through the center of the cylindrical part (*open circles*) and the spherical part (*closed circles*), respectively. The arrows in the insets represent the direction of the lines. The metabolite concentrations were as depicted in Table 1.

relay chains such as the PTS. Yet, the results are as good as can be obtained with the current knowledge of this type of system, and the glucose-PTS of *E. coli* is one of the best studied systems of its sort. The parameter values we used did not result from fitting procedures, in line with the silicon cell philosophy (Westerhoff, 2001). Therefore, our results are the mere implications of the biochemical knowledge of the system that exists today. It should be noted that as our biochemical knowledge continues to progress, our results may develop further.

APPENDIX: SPHERICAL VERSUS ROD-LIKE MODEL CELL

We modeled *E. coli* as a cylinder, with a diameter of 1.2 μm ($r = 0.6$ μm) and a length of 1.8 μm, closed on both sides by half a sphere, with radius 0.6 μm, and as a sphere with a radius of 0.6 μm (as described by Blom and Peletier, 2000, 2002). For the first rod-shaped cell we included lateral diffusion of the membrane components in the model. The diffusion coefficient for the lateral diffusion of the $IICB^{Glc}$-related enzyme species was assumed to be 0.2 $\mu m^2\ s^{-1}$ (Vrljic et al., 2002). The other parameter values were chosen as described in the main text. In the rod cell we assumed rotational symmetry around the long axis and mirror symmetry with respect to the plane through the center of the cell perpendicular to the long axis. The solutions in the spherical model cell showed spherical symmetry. To describe the behavior of the PTS in both model cells, we considered the concentrations of the enzyme species along a line with length equal to r perpendicular to the surface. At high glucose and PEP concentrations, we found that in the rod cell the concentration distribution of the different enzyme species along such lines varied slightly depending on the position in the rod, the difference in concentration gradients not amounting to more than 2% in most cases and being always smaller than 6%. The concentrations of the various enzyme species found along the radius of the spherical cell lay approximately in between the extremes found in the rod, with the exception of nonphosphorylated IIA^{Glc}. The concentration gradients were therefore always somewhat smaller, but in general the deviations between the gradients found in the spherical cells and those in the rod-like cells were $<2\%$ and at most 11%, again in case of nonphosphorylated IIA^{Glc}. In the rod, hardly any membrane gradients developed in $IICB^{Glc}$-related species and the difference in glucose influx between the rod and the sphere was smaller than 1%. The above applied to all cases we studied, e.g., using other

metabolite concentrations or membrane diffusion coefficients; the effect on the flux and concentration distribution of a hundredfold decrease in the membrane diffusion coefficient was $<1‰$. The difference between the gradients in the rod cell and the spherical cell at high flux are illustrated in Fig. 5, which shows the two cases with the largest deviations. It is clear from Fig. 5 that for the behavior of the PTS, the differences between a rod and a spherical cell are only marginal.

The authors thank Drs C.L. Woldringh, J.M. Rohwer, R. van Driel, K.J. Hellingwerf, B.N. Kholodenko, and the reviewers for thoughtful comments, and H. Brinkman for his contribution to the work.

The work was supported via the ICES-KIS II program.

REFERENCES

Blom, J. G., and M. A. Peletier. 2000. Diffusive gradients in the PTS system. Report MAS-R0020. CWI, Amsterdam (http://www.cwi.nl/cwi/publications_bibl/).

Blom, J. G., and M. A. Peletier. 2002. The importance of being cigar-shaped. Report MAS-R0228. CWI, Amsterdam (http://www.cwi.nl/cwi/publications_bibl/).

Botsford, J. L., and J. G. Harman. 1992. Cyclic AMP in prokaryotes. *Microbiol. Rev.* 56:100–122.

Brown, G. C., and B. N. Kholodenko. 1999. Spatial gradients of cellular phospho-proteins. *FEBS Lett.* 457:452–454.

Dayel, M. J., E. F. Hom, and A. S. Verkman. 1999. Diffusion of green fluorescent protein in the aqueous-phase lumen of endoplasmic reticulum. *Biophys. J.* 76:2843–2851.

de Reuse, H., and A. Danchin. 1988. The ptsH, ptsI, and crr genes of the *Escherichia coli* phosphoenolpyruvate-dependent phosphotransferase system: a complex operon with several modes of transcription. *J. Bacteriol.* 170:3827–3837.

Elowitz, M. B., M. G. Surette, P. E. Wolf, J. B. Stock, and S. Leibler. 1999. Protein mobility in the cytoplasm of *Escherichia coli*. *J. Bacteriol.* 181:197–203.

Francke, C., H. V. Westerhoff, J. G. Blom, and M. A. Peletier. 2002. Flux control of the bacterial phosphoenolpyruvate:glucose phosphotransferase system and the effect of diffusion. *Mol. Biol. Rep.* 29:21–26.

Goldbeter, A., and D. E. Koshland, Jr. 1982. Sensitivity amplification in biochemical systems. *Q. Rev. Biophys.* 15:555–591.

Gordon, R. E. 1974. The genus *Bacillus*. *In* Handbook of Microbiology, condensed edition. A. I. Laskin, and H. A. Lechevalier, editors. CRC Press, Cleveland, Ohio. 65–82.

Hogema, B. M., J. C. Arents, R. Bader, K. Eijkemans, H. Yoshida, H. Takahashi, H. Aiba, and P. W. Postma. 1998. Inducer exclusion in *Escherichia coli* by non-PTS substrates: the role of the PEP to pyruvate ratio in determining the phosphorylation state of enzyme IIA^{Glc}. *Mol. Microbiol.* 30:487–498.

Kholodenko, B. N., G. C. Brown, and J. B. Hoek. 2000. Diffusion control of protein phosphorylation in signal transduction pathways. *Biochem. J.* 350:901–907.

Kundig, W., S. Gosh, and S. Roseman. 1964. Phosphate bound to histidine in a protein as intermediate in a novel phosphotransferase system. *Proc. Natl. Acad. Sci. USA.* 52:1067–1074.

Lee, S. J., W. Boos, J. P. Bouche, and J. Plumbridge. 2000. Signal transduction between a membrane-bound transporter, PtsG, and a soluble transcription factor, Mlc, of *Escherichia coli*. *EMBO J.* 19:5353–5361.

Lengeler, J. W., and K. Jahreis. 1996. Phosphotransferase Systems or PTSs as Carbohydrate Transport and as Signal Transduction Systems. *In* Handbook of Biological Physics, Vol. 2. W. N. Konings, H. R. Kaback, and J. S. Lolkema, editors. Elsevier Science B.V., Amsterdam. 573–598.

Lux, R., V. R. Munasinghe, F. Castellano, J. W. Lengeler, J. E. Corrie, and S. Khan. 1999. Elucidation of a PTS-carbohydrate chemotactic signal pathway in *Escherichia coli* using a time-resolved behavioral assay. *Mol. Biol. Cell.* 10:1133–1146.

Makman, R. S., and E. W. Sutherland. 1965. Adenosine 3′,5′-phosphate in *Escherichia coli*. *J. Biol. Chem.* 240:1309–1314.

Meadow, N. D., D. K. Fox, and S. Roseman. 1990. The bacterial phosphoenolpyruvate:glycose phosphotransferase system. *Annu. Rev. Biochem.* 59:497–542.

Misko, T. P., W. J. Mitchell, N. D. Meadow, and S. Roseman. 1987. Sugar transport by the bacterial phosphotransferase system. Reconstitution of inducer exclusion in *Salmonella typhimurium* membrane vesicles. *J. Biol. Chem.* 262:16261–16266.

Nanninga, N. 1998. Morphogenesis of *Escherichia coli*. *Microbiol. Mol. Biol. Rev.* 62:110–129.

Nelson, S. O., B. J. Scholte, and P. W. Postma. 1982. Phosphoenolpyruvate:sugar phosphotransferase system-mediated regulation of carbohydrate metabolism in *Salmonella typhimurium*. *J. Bacteriol.* 150:604–615.

Novotny, M. J., W. L. Frederickson, E. B. Waygood, and M. H. Saier, Jr. 1985. Allosteric regulation of glycerol kinase by enzyme III^{Glc} of the phosphotransferase system in *Escherichia coli* and *Salmonella typhimurium*. *J. Bacteriol.* 162:810–816.

Ortega, F., L. Acerenza, H. V. Westerhoff, F. Mas, and M. Cascante. 2002. Product dependence and bifunctionality compromise the ultrasensitivity of signal transduction cascades. *Proc. Natl. Acad. Sci. USA.* 99:1170–1175.

Osumi, T., and M. H. Saier, Jr. 1982. Regulation of lactose permease activity by the phosphoenolpyruvate:sugar phosphotransferase system: evidence for direct binding of the glucose-specific enzyme III to the lactose permease. *Proc. Natl. Acad. Sci. USA.* 79:1457–1461.

Postma, P. W., W. Epstein, A. R. Schuitema, and S. O. Nelson. 1984. Interaction between III^{Glc} of the phosphoenolpyruvate:sugar phosphotransferase system and glycerol kinase of *Salmonella typhimurium*. *J. Bacteriol.* 158:351–353.

Postma, P. W., J. W. Lengeler, and G. R. Jacobson. 1993. Phosphoenolpyruvate:carbohydrate phosphotransferase systems of bacteria. *Microbiol. Rev.* 57:543–594.

Robillard, G. T., and J. Broos. 1999. Structure/function studies on the bacterial carbohydrate transporters, enzymes II, of the phosphoenolpyruvate-dependent phosphotransferase system. *Biochim. Biophys. Acta.* 1422:73–104.

Rohwer, J. M., R. Bader, H. V. Westerhoff, and P. W. Postma. 1998a. Limits to inducer exclusion: inhibition of the bacterial phosphotransferase system by glycerol kinase. *Mol. Microbiol.* 29:641–652.

Rohwer, J. M., P. W. Postma, B. N. Kholodenko, and H. V. Westerhoff. 1998b. Implications of macromolecular crowding for signal transduction and metabolite channeling. *Proc. Natl. Acad. Sci. USA.* 95:10547–10552.

Rohwer, J. M., P. R. Jensen, Y. Shinohara, P. W. Postma, and H. V. Westerhoff. 1996. Changes in the cellular energy state affect the activity of the bacterial phosphotransferase system. *Eur. J. Biochem.* 235:225–230.

Rohwer, J. M., N. D. Meadow, S. Roseman, H. V. Westerhoff, and P. W. Postma. 2000. Understanding glucose transport by the bacterial phosphoenolpyruvate:glycose phosphotransferase system on the basis of kinetic measurements in vitro. *J. Biol. Chem.* 275:34909–34921.

Saier, M. H., Jr., B. U. Feucht, and M. T. McCaman. 1975. Regulation of intracellular adenosine cyclic 3′:5′ monophosphate levels in *Escherichia coli* and *Salmonella typhimurium*. Evidence for energy-dependent excretion of the cyclic nucleotide. *J. Biol. Chem.* 250:7593–7601.

Saier, M. H., Jr., M. J. Novotny, D. Comeau-Fuhrman, T. Osumi, and J. D. Desai. 1983. Cooperative binding of the sugar substrates and allosteric regulatory protein (enzyme III^{Glc} of the phosphotransferase system) to the lactose and melibiose permeases in *Escherichia coli* and *Salmonella typhimurium*. *J. Bacteriol.* 155:1351–1357.

Saier, M. H., Jr., T. M. Ramseier, and J. Reizer. 1996. Regulation of carbon utilization. *In* Escherichia coli and Salmonella cellular and Molecular Biology, 2nd ed, Vol 1. F. C. Neidhardt, editor. ASM press, Washington, D.C. 1325–1343.

Seok, Y. J., M. Sondej, P. Badawi, M. S. Lewis, M. C. Briggs, H. Jaffe, and A. Peterkofsky. 1997. High affinity binding and allosteric regulation of *Escherichia coli* glycogen phosphorylase by the histidine phosphocarrier protein, HPr. *J. Biol. Chem.* 272:26511–26521.

Sherman, F. 1991. Getting started with yeast. *Methods Enzymol.* 194:3–21.

Stülke, J., and W. Hillen. 1999. Carbon catabolite repression in bacteria. *Curr. Opin. Microbiol.* 2:195–201.

Tanaka, Y., K. Kimata, and H. Aiba. 2000. A novel regulatory role of glucose transporter of *Escherichia coli*: membrane sequestration of a global repressor Mlc. *EMBO J.* 19:5344–5352.

van der Vlag, J., K. van Dam, and P. W. Postma. 1994. Quantification of the regulation of glycerol and maltose metabolism by IIA^{Glc} of the phosphoenolpyruvate-dependent glucose phosphotransferase system in *Salmonella typhimurium*. *J. Bacteriol.* 176:3518–3526.

van der Vlag, J., R. van't Hof, K. van Dam, and P. W. Postma.1995. Control of glucose metabolism by the enzymes of the glucose phosphotransferase system in *Salmonella typhimurium*. *Eur. J. Biochem.* 230:170–182.

Voegele, R. T., G. D. Sweet, and W. Boos. 1993. Glycerol kinase of *Escherichia coli* is activated by interaction with the glycerol facilitator. *J. Bacteriol.* 175:1087–1094.

Vrljic, M., S. Y. Nishimura, S. Brasselet, W. E. Moerner, and H. M. Mc Connell. 2002. Translational diffusion of individual class II MHC membrane proteins in cells. *Biophys. J.* 83:2681–2692.

Weigel, N., M. A. Kukuruzinska, A. Nakazawa, E. B. Waygood, and S. Roseman. 1982. Sugar transport by the bacterial phosphotransferase system. Phosphoryl transfer reactions catalyzed by enzyme I of *Salmonella typhimurium*. *J. Biol. Chem.* 257:14477–14491.

Weast, R. C. (editor). 1975. Handbook of Chemistry and Physics. 55th ed. CRC Press, Cleveland, Ohio.

Westerhoff, H. V. 2001. The silicon cell. Not dead but live! *Metab. Eng.* 3:207–210.

Woldringh, C. L., and N. Nanninga. 1985. Structure of nucleoid and cytoplasm in the intact cell. *In* Molecular Cytology of Escherichia coli. N. Nanninga, editor. Academic Press, London and New York. 161–197.